Journal of Medicinal Chemistry

Article

pubs.acs.org/jmc

Novel Toll-like Receptor 2 Ligands for Targeted Pancreatic Cancer Imaging and Immunotherapy

Amanda Shanks Huynh,[†] Woo Jin Chung,[§] Hyun-Il Cho,[‡] Valerie E. Moberg,[†] Esteban Celis,[‡] David L. Morse,*[,†] and Josef Vagner*[,§]

[†]Department of Cancer Imaging and Metabolism and [‡]Department of Immunology, H. Lee Moffitt Cancer Center and Research Institute, 12902 Magnolia Drive, Tampa, Florida 33612, United States

[§]The BIO5 Research Institute, University of Arizona, 1657 E. Helen Street, Tucson, Arizona 85721, United States

Supporting Information

ABSTRACT: Toll-like receptor 2 (TLR2) is a target for immune system stimulation during cancer immunotherapy and a cell-surface marker for pancreatic cancer. To develop targeted agents for cancer imaging and therapy, we designed, synthesized, and characterized 13 novel, fully synthetic high affinity TLR2 agonists. Analogue **10** had the highest agonist activity (NF-κB functional assay, EC_{50} = 20 nM) and binding affinity (competitive binding assay, K_i = 25 nM). As an immune adjuvant, compound **10** stimulated the immune system in vivo by generation and persistence of antigen-specific CD8+ T cells indicating its potential use in cancer immunotherapy. After conjugation of near-infrared dye to **10**, agonist activity (EC_{50} = 34 nM) and binding affinity (K_i = 11 nM) were retained in **13**. Fluorescence signal was present in TLR2 expressing pancreatic tumor xenografts 24 h after injection of **13**, while an excess of unlabeled ligand blocked **13** from binding to the tumor, resulting in significantly decreased signal ($p < 0.001$) demonstrating in vivo selectivity.

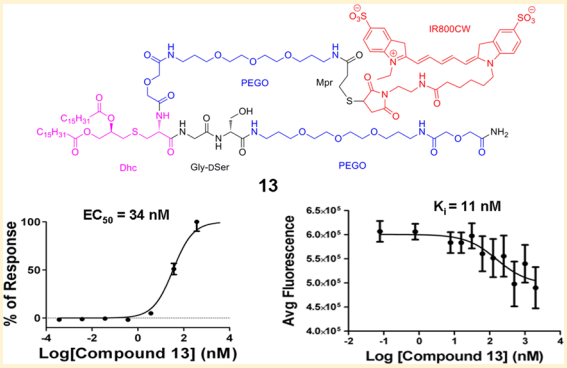

INTRODUCTION

The discovery of ligands and small molecule synthetic compounds that specifically activate Toll-like receptor 2 (TLR2) has raised interest in this cell-surface receptor as a potential target for the development of new therapies, including the treatment of cancer.[1] TLR2 has a role in activation and regulation of the innate immune system, and targeted stimulation of this receptor has been used to augment cancer immunotherapy.[1b,2] Although TLR2 is predominantly expressed in tissues involved in immune function, the expression profile varies among tissues and cell types.[3] TLR2 is a type I transmembrane glycoprotein characterized by an external antigen recognition domain comprising a highly conserved leucine-rich repeat motif, a transmembrane domain, and a cytoplasmic Toll/interleukin-1 (TIR) receptor homology signaling domain. Intracellular signaling is activated by agonist binding and is facilitated by the formation of the cytoplasmic TIR domain through heterodimerization with either TLR1 or TLR6.[4] TLR2 is a pattern recognition receptor with the ability to recognize pathogen-associated molecular patterns (PAMPs).[5] Stimulation by PAMPs initiates signaling cascades that activate NF-κB transcription factors inducing the secretion of proinflammatory cytokines and effector cytokines directing the immune response.[5c]

The potential use of synthetic TLR2 agonists for the enhancement of cancer immunotherapy is an active area of research.[6] There are four mechanisms by which TLR2 stimulation may produce significant antitumor activity: enhancement of the innate immunity, enhancement of T-cell immunity, enhancement of cytotoxic antibody function, and induction of apoptosis in TLR2-positive tumors.[1b] Examples include the TLR2 induction of tumor necrosis factor-α (TNF-α), increasing the production of nitric oxide synthase (iNOS) and thus inducing apoptosis of chemotherapy-resistant tumor cells,[7] reduction of bladder tumor growth by TLR2 agonist SMP-105,[8] and a combination therapy of macrophage-activating lipopeptide 2 kDa (MALP-2) and gemcitabine that increased the survival rates of incompletely resectable pancreatic cancers in a phase I/II trial.[9] We have previously reported the use of TLR agonists as immune adjuvants that can increase the magnitude and duration of peptide vaccine-induced T cell responses,[10] as demonstrated by our TriVax vaccine that elicits potent protective antitumor immunity as well as remarkable therapeutic effects against melanoma.[11]

In an effort to improve the less than 6% 5-year survival rate for pancreatic cancer,[12] we are investigating the potential of TLR2 ligands for use in targeted pancreatic cancer imaging and treatment. Improved survival rates are associated with the surgical resection of the primary tumor if the tumor tissue is

Received: July 10, 2012
Published: October 25, 2012

   dx.doi.org/10.1021/jm301002f | J. Med. Chem. 2012, 55, 9751−9762

Table 1. Synthesized Compounds

compd	X, Y, or Z modification	MW calcd/found[a]
	X-Cys(*S*-[2,3-bis(palmitoyl)oxy-(*R*)-propyl])-Gly-Asn-Asn-Asp-Glu-Ser-Asn-Ile-Ser-Phe-Lys-Glu-Lys-NH_2	
1	palmitoyl-	2371.4/1186.23 $(M + 2)^+$
2	fluorescein-	2491.3/2492.36
3	Ac-PEGO[b]-	2493.4/2494.43
4	Ac-Aha[c]-	2288.3/2288.0
5	adapalenoyl-	2526.4/2528.40
6	Ac-Aun[d]-	2358.4/2359.41
7	tretinoyl-	2414.4/2415.28
	Ac-PEGO-Cys(*S*-[2,3-bis(palmitoyl)oxy-(*R*)-propyl])-Y	
8[e]	-Ser-Arg-Phe-Asp-Glu-Asp-Asp-Leu-Glu-NH_2	2137.2/1069.90 $(M + 2)^{2+}$
9	-Gly-Ser-Gln-Asn-Leu-Ala-Ser-Leu-Glu-Glu-NH_2	2059.2/1030.3 $(M + 2)^{2+}$
10	-Gly-DSer-PEGO-NH_2	1492.95/1493.5
	Z-PEGO-Cys(*S*-[2,3-bis(palmitoyl)oxy-(*R*)-propyl])-Gly-DSer-PEGO-NH_2	
11	Eu-DTPA[f]-	1975.98/1975.4−1977.4
12	Mpr[g]-	1538.95/1539.5
13	IRDye800CW-Mpr-	2728.8/1330.60 $(M + 2)^{2+}$

[a]Found = as determined by mass spectrometery. [b]PEGO denotes 20-atom ethylene glycol oligomer (the full structure is depicted in the Supporting Information). [c]Aha denotes 6-aminohexanoyl residue. [d]Aun denotes 11-aminoundecanoyl residue. [e]All amino acid residues are D-configuration. [f]Eu-DTPA denotes europium chelated in diethylenetriaminepentaacetic acid. [g]Mpr denotes 3-mercaptopropionyl residue.

completely removed at the margins.[13] However, it is a high risk procedure with a low success rate due to difficulty in clearly identifying tumor tissue from normal tissue, resulting in positive resection margins (R_1).[14] The development of new intraoperative surgical methods employing fluorescence guided tumor detection could lead to increased negative resection margins (R_0) resulting in improved survival rates. Recent clinical studies involving image-guided surgeries have demonstrated the potential of this approach.[15] We have previously reported TLR2 as a bona fide cell surface marker for pancreatic cancer that is highly expressed in 70% of pancreatic tumors but is not highly expressed in surrounding normal pancreas tissue.[16] Fluorescence imaging probes developed using TLR2 specific ligands could be applied to the intraoperative detection of pancreatic tumor margins.

A variety of microbial component derived lipopeptides (LPs) are recognized as TLR2 ligands. For example, mycoplasma produce diacylated MALP-2, Cys(*S*-[2,3-bisacyloxy-(*R*)-propyl])-Gly-Asn-Asn-Asp-Glu-Ser-Asn-Ile-Ser-Phe-Lys-Glu-Lys, which binds to the TLR2/TLR6 heterodimer.[17] The structure−activity relationships (SAR) of TLR2 binding and stimulation of the immune system for many synthetic LPs are well documented in the literature. Both the well-characterized synthetic di- and triacylated LP ligands, Pam_2CSK_4 and Pam_3CSK_4, bind to internal protein pockets through hydrophilic interactions to selectively induce signaling via the TLR2/TLR6 and TLR2/TLR1 heterodimers, respectively.[4b,17c,18] In addition to LPs, the serum amyloid A protein (SAA) was recently identified as a potent TLR2 agonist by Cheng et al. and is a major acute-phase protein that is considered to be a marker for inflammatory diseases.[1a,19]

TLR2 specific agonist ligands developed herein have potential for use in both the development of targeted agents for the imaging and treatment of pancreatic cancer and as an adjuvant for cancer immunotherapy. In an effort to identify novel TLR2 ligands that are highly potent TLR2 agonists for use in immunotherapy, or ligands with high binding affinity for TLR2 with potential for attachment of imaging contrast and therapeutic agents, we have iteratively synthesized two sets of rationally designed synthetic compounds and investigated their SAR by in vitro functional bioassays, in cyto binding assays, in vivo immune system stimulation, and molecular imaging studies demonstrating tumor specificity. From the crystal structure of TLR2 complexes, it is known that the minimal ligand recognition structure contains a Cys(*S*-[2,3-bis(palmitoyl)oxy-(*R*)-propyl] residue.[18d] Therefore, we kept this pharmacophore element and made changes to the flexible peptide component. The rationale behind this design strategy was to remove the metabolically unstable peptide and the positively charged tetralysine moiety and substitute them with indifferent and hydrophobic polyethylene glycol chains. The goal of this design strategy was to discover water-soluble ligands without compromising potency, and this was achieved for compounds **10**, **11**, and **13** (vide infra). Compound **10** has potent bioactivity (EC_{50} = 20 nM), high affinity binding (K_i = 25 nM), and effective immune system stimulation. After conjugation of a near-infrared fluorescent dye to **10** generating **13**, high bioactivity (EC_{50} = 34 nM) and binding affinity (K_i = 11 nM) were retained, and tumor specificity was observed in vivo by fluorescence imaging of mice bearing TLR2 expressing tumor xenografts. In addition, **10** has a greatly simplified synthesis strategy with improved solubility and a built-in attachment point for imaging contrast and/or a therapeutic moiety.

RESULTS

TLR2 Ligand Library Design and Synthesis. Thirteen novel fully synthetic compounds were designed and synthesized to discover novel TLR2 specific ligands with the desired properties of high specificity, high agonist activity, high binding affinity, solubility, and built-in attachment points for conjugation of fluorescent dyes and chelates. Initially, seven compounds (**1**−**7**) based on the structure of the bispalmitoylated MALP-2,[17a] Cys(*S*-[2,3-bis(palmitoyl)oxy-(*R*)-propyl])-Gly-Asn-Asn-Asp-Glu-Ser-Asn-Ile-Ser-Phe-Lys-Glu-Lys, were synthesized. Each compound in the set comprised the same scaffold, X-Cys(*S*-[2,3-bis(palmitoyl)oxy-(*R*)-propyl])-Gly-Asn-Asn-Asp-Glu-Ser-Asn-Ile-Ser-Phe-Lys-Glu-Lys-NH_2, or X-MALP-2, where the X-group represents an N-terminal modification (Table 1, Supporting Information Figure 5).

dx.doi.org/10.1021/jm301002f | J. Med. Chem. 2012, 55, 9751−9762

Scheme 1. Synthetic Route for Eu-DTPA Compound 11, Mpr Compound 12, and IRDye800CW Compound 13[a]

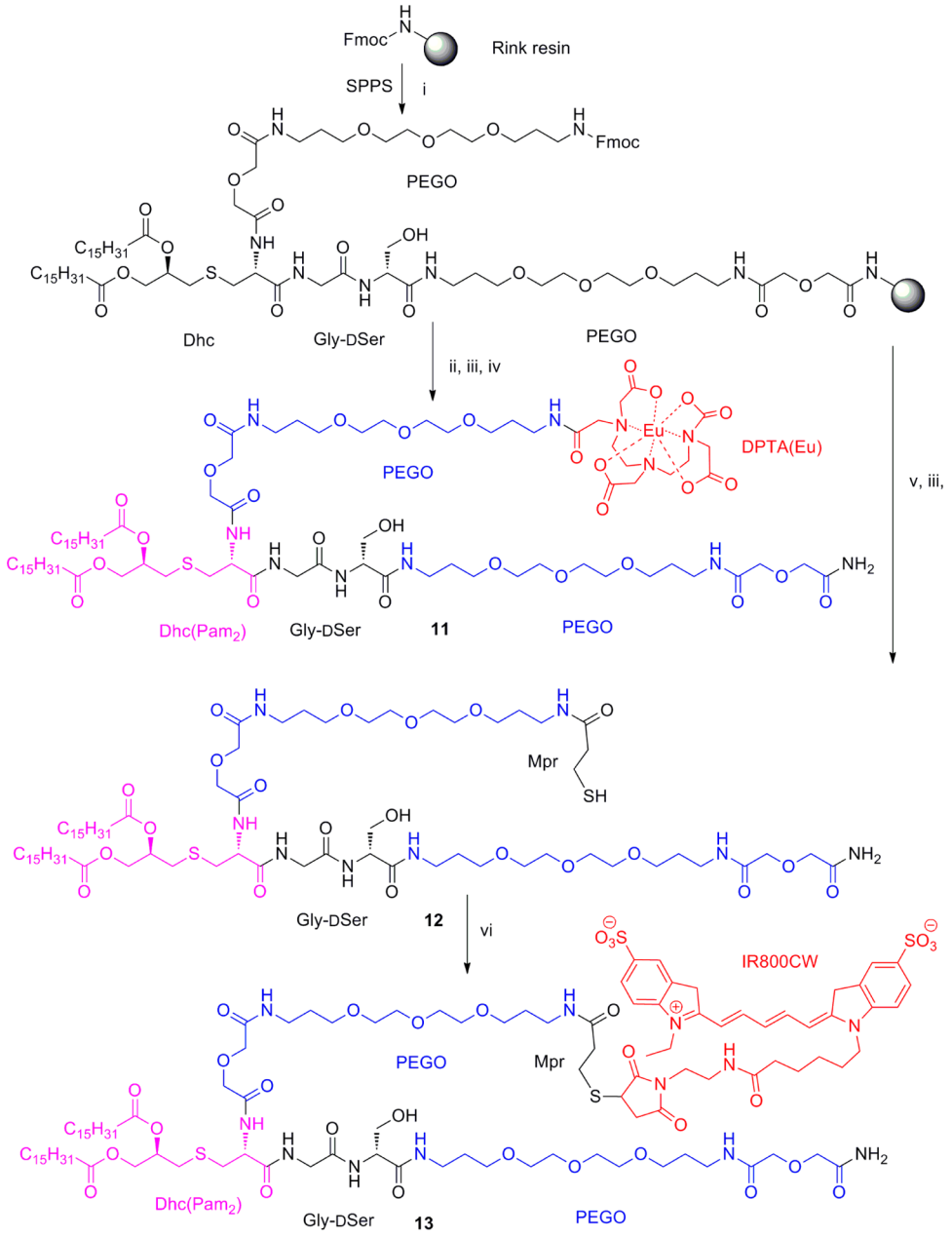

[a](i) Fmoc/*t*-Bu synthesis continued as follows: (a) piperidine/DMF (1:4) for Fmoc deprotection; (b) Fmoc-aa-OH (3 equiv), HOBt (3 equiv), DIEA (6 equiv), and HBTU (3 equiv) in DMF for amino acid couplings. (ii) DTPA was attached after Fmoc deprotection as follows: (a) DTPA anhydride (3 equiv) and HOBt (3 equiv) were dissolved in dry DMSO (0.5M), heated to 60 °C for 3 min and then stirred at room temperature for 30 min. (b) Preformed DTPA-OBt diester mixture reacts with the resin overnight. (iii) TFA-scavenger cocktail (90% trifluoroacetic acid, 5% water, 5% triisopropylsilane) for 2 h. (iv) Eu(III)Cl_3 (3.0 equiv) in 0.1 M ammonium acetate buffer, pH 8.0, overnight. (v) (a) Piperidine/DMF (1:4) for Fmoc deprotection; (b) Trt-3-mercaptopropionic acid (3 equiv), DIEA (6 equiv), and HBTU (3 equiv) in DMF. (vi) IRDye800CW maleimide (1 equiv) in DMF.

After compounds **1**–**7** were screened for bioactivity (vide infra), a second set of three analogues (**8**–**10**) was designed based on SAR knowledge gained from the first set. The scaffold, Ac-PEGO-Cys(*S*-[2,3-bis(palmitoyl)oxy-(*R*)-propyl])-Y, was derived using compound **3**'s N-terminal modification of the MALP-2 LP that included an acetylated 20-atom ethylene glycol oligomer (PEGO) plus Y modifications at the C-terminus (Table 1). Compound **8**'s Y-group modification was derived from a CD14 peptide known to induce the physical proximity of CD14, TLR2, and TLR1.[20] Compound **9**'s Y-group modification was derived from a *S. aureus* peptide that should be more acidic or at least neutral compared to the recently identified potent TLR2 agonist serum amyloid A (SAA) by Cheng et al.[1a,21] To test the importance of the peptide component of MALP-2 in terms of potency, compound **10**'s Y-group modification was derived from compound **3**'s structure with the peptide component reduced to a short Gly-DSer linker with a PEGO-NH_2 at the C-terminus to enhance solubility.

Since compound **10** was determined to have the most potent TLR2 bioactivity (vide infra), three final compounds were

dx.doi.org/10.1021/jm301002f | *J. Med. Chem.* 2012, 55, 9751–9762

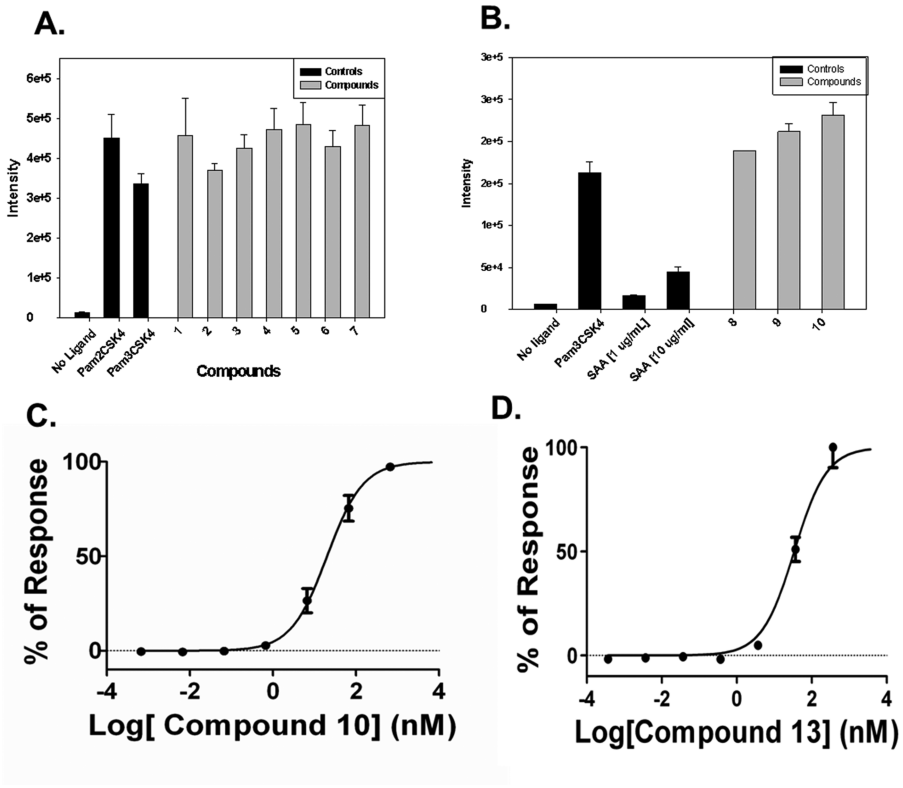

Figure 1. Screening of (A) X-Cys(*S*-[2,3-bis(palmitoyl)oxy-(*R*)-propyl])-MALP-2 derived peptide library (compounds **1**−**7**) and (B) analogues (**8**-**10**) with an Ac-PEGO-Cys(*S*-[2,3-bis(palmitoyl)oxy-(*R*)-propyl])-Y and SAA for TLR2 agonist activity determined using the functional bioassay. All compounds exhibit high luminescence intensities similar to the TLR2 agonist controls, Pam_2CSK_4 and Pam_3CSK_4, using the HEK-293/hTLR2 cells (n = 3 assays with quadruplicate wells, $p < 0.0003$). Dose−response curves were generated by measuring the TLR2 agonistic activity for (C) compound **10** and (D) compound **13**. Experiments were performed by serially adding (0.001 ng/mL to 10 μg/mL) compound to HEK-293/hTLR2 expressing cells (n > 3 assays with quadruplicate wells, $R^2 > 0.98$).

designed and synthesized to incorporate at the N-terminus, in lieu of the acetyl group, a europium diethylenetriaminepentaacetic acid (Eu-DTPA) chelate (compound **11**), 3-mercaptopropionyl residue (Mpr) for attachment to thiol groups (compound **12**), and the near-infrared dye IRDye800CW (LI-COR, Lincoln, NE, U.S.) functionalized with Mpr for attachment (compound **13**) (Scheme 1, Table 1). Compound **11** was used to determine TLR2 binding affinity via in cyto time-resolved fluorescence (TRF) binding assays. Compound **13** was used for in vivo fluorescence imaging to determine TLR2 specificity and binding.

In Vitro Functional Bioassay. We developed a functional bioactivity assay to specifically detect intracellular signaling induced by agonist stimulation of the human TLR2 receptor at the cell surface. This assay underwent optimization prior to starting our peptide screenings. Optimal NF-κB induced expression of luciferase led to observed luminescence 48 h after transient transfection and 24 h after ligand stimulation. Luminescence intensity was significantly greater (50-fold, $n = 6$, $p < 0.001$) in Pam_3CSK_4 ligand stimulated HEK-293/hTLR2 cells relative to cells incubated with no ligand (Supporting Information Figure 1C). The ligand-stimulated parental HEK-293 cells had no measurable luminescence. Hence, the measured luminescence is specifically induced by signaling of TLR2 agonists via the NF-κB pathway.

We initially screened the first set of seven MALP-2 derived compounds (**1**−**7**) with N-terminal modifications (Table 1) to determine in vitro TLR2 agonist activity. All seven of the compounds exhibited comparable levels of NF-κB induced luminescence relative to the reference TLR2 agonist ligand controls (Figure 1A). The control, Pam_2CSK_4, is a synthetic diacylated lipopeptide with the same palmitic acid pharmacophore moiety (Pam2 (*S*-[2,3-bis(palmitoyloxy)-(*R*)-propyl])) found in MALP-2. All seven of the compounds elicited an agonist response comparable to that of Pam_2CSK_4 in the screening assay using the 1 μg/mL concentration.

A second set of analogues (**8**−**10**) that retained the N-terminal modification of compound **3**, acetylated PEGO, with different C-terminal variations were screened for TLR2 agonist activity (Table 1). All three of the compounds exhibited significant luminescence intensity relative to the no-ligand control, comparable to the Pam_3CSK_4 positive control and significantly more potent than SAA at both 1 and 10 μg/mL ($n = 4$, $p < 0.001$) (Figure 1B). The fold of enhancement for **8**, **9**, and **10** vs SAA at 1 μg/mL was 11, 13, and 14, respectively. The fold of enhancement for **8**, **9**, and **10** at 1 μg/mL vs SAA at 10 μg/mL was 4.2, 4.8, and 5.2, respectively.

The agonist potency of compounds **3**, **8**−**13**, Pam_2CSK_4, and Pam_3CSK_4 was characterized over a range of concentrations (0.001 ng/mL to 10 μg/mL) to determine EC_{50} values. The resulting normalized dose−response curves generated by measuring the TLR2 agonistic activity for each compound and EC_{50} values are reported in Table 2 (n = 6 assays for test compounds and n = 3 assays for control compounds, $R^2 > 0.94$) (Supporting Information Figure 2). Test compounds (**3**, **8**−**10**) are potent TLR2 agonists with low nanomolar EC_{50} values ranging from 20 to 78 nM. Compound **10** had the lowest EC_{50} (20 nM) (Figure 1C), which is comparable to the EC_{50} values for

dx.doi.org/10.1021/jm301002f | J. Med. Chem. 2012, 55, 9751−9762

Table 2. TLR2 Agonist Activity (EC_{50}) Calculated from Dose-Response Curves

compd	EC_{50} (nM)	std error	R^2
3	56	1.1	0.99
8	25	1.1	0.99
9	78	1.1	0.99
10	20	1.0	0.99
11	204	1.3	0.97
12	39	1.1	0.98
13	34	1.2	0.98
Pam_2CSK_4	3.7	1.4	0.96
Pam_3CSK_4	23	1.5	0.94

Pam_2CSK_4 (3.7 nM) and Pam_3CSK_4 (23 nM) positive controls (Supporting Information Figure 2F and 2G). Compounds **11**, **12**, and **13** based on the structure of **10** with N-terminal attachments were determined to retain nanomolar TLR2 agonist activity, 204, 39, and 34 nM, respectively (Table 2, Figure 1D, Supporting Information Figure 2D,E).

In Cyto Binding Assays. Lanthanide-based time-resolved fluorescence (TRF) saturation binding and competition binding assays were performed using TLR2 expressing cell lines. Saturation binding assays determined that the K_d for the Eu-DTPA chelate labeled compound **11** was 34, 74, and 78 nM and B_{max} was 114 271, 269 878, and 951 170 AFU for the HEK-293/hTLR2, SU.86.86, and Capan-I cells, respectively ($n > 3$ assays per cell line, $R^2 > 0.96$) (Table 3, Figure 2A, and Supporting Information Figure 3). Competitive binding assays using compound **11** as the competing ligand determined that the K_i for compounds **10** and **13** is 25 and 11 nM in the HEK-293/hTLR2 cell line, respectively, and 91 and 67 nM in the SU.86.86 cell line ($n > 4$ assays, $R^2 > 0.78$) (Table 4, Figure 2B,C, and Supporting Information Figure 4A,C). Compound **12** exhibited the highest binding affinity in the SU.86.86 cell line with a K_i of 25 nM ($n = 4$ assays, $R^2 = 0.90$) (Supporting Information Figure 4B).

Table 3. TLR2 Binding Affinity (K_d) for Compound 11 Determined by Saturation Binding Assays

TLR2 expressing cell line	K_d (nM)	std error	B_{max} (AFU)	std error	R^2
HEK-293/hTLR2	34	13	114 271	17 001	0.97
SU.86.86	74	16	269 878	28 809	0.99
Capan-I	78	22	951 170	112 968	0.96

In Vivo Immune Response. Compound **10** was evaluated in vivo as an immune adjuvant using TriVax. This peptide vaccine, comprising synthetic peptide representing CD8+ T cell epitopes ($Trp1_{455/9M}$), TLR agonists that function as potent immunologic adjuvants (compound **10**, Pam_2CSK_4, or Pam_3CSK_4), and co-stimulatory anti-CD40 monoclonal antibody (Clone, FGk-45.5) to generate large numbers of antigen-specific CD8+ T cells capable of recognizing and killing tumor cells.[11,12] For comparison, the well-characterized commercially available synthetic TLR2 agonists, Pam_2CSK_4 and Pam_3CSK_4, were also evaluated for their ability to function as immulogic adjuvants of this peptide vaccine. The activity of each compound as an immune adjuvant was evaluated in vivo by measuring the $Trp1_{455/9M}$-specific CD8+ T cell responses in the blood on days 7, 21, and 34 after immunization by flow cytometry analysis ($n = 3$) (Figure 3A). $Trp1_{455/9M}$, a TLR agonist, was tested using the TLR2 functional bioassay and is not a TLR2 agonist (data not shown). The maximum amount of fluorescently stained tetramer positive CD8+ T cells for **10**, Pam_2CSK_4, and Pam_3CSK_4 observed on day 7 was 49.6%, 56.6%, and 51.7%, respectively. The 100% response rate of the tetramer positive CD8+ T cells using **10** as the immune adjuvant observed on day 7 decreased to an average of 25.7% on day 21 and 12.7% on day 34, which were comparable responses to using either Pam_2CSK_4 or Pam_3CSK_4 (Figure 3B). Therefore these results indicate that compound **10** exhibited activity similar to those of the other known TLR2 agonists, Pam_2CSK_4 and Pam_3CSK_4, for the generation and persistence of antigen-specific CD8+ T cells. No signs or symptoms of stress or toxicity were observed in the mice over the course of the experiment.

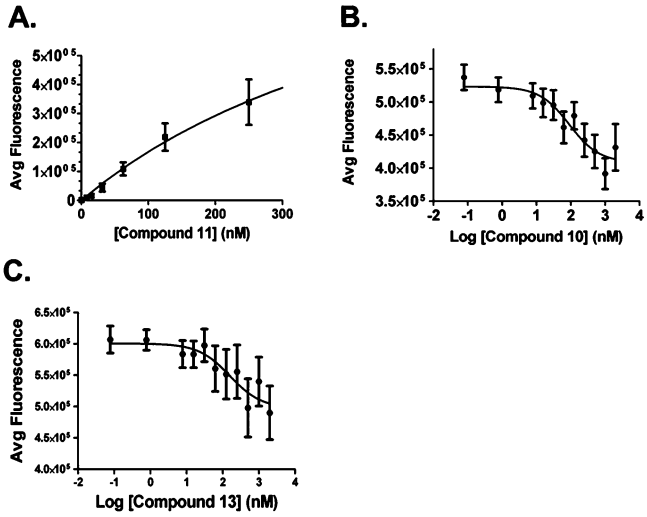

Figure 2. Mean binding analysis curves generated by in cyto TRF binding assays. (A) Saturation binding curve shows the specific binding (total − nonspecific) curve of Eu-DTPA-labeled compound **11** to TLR2 using HEK-293/hTLR2 cells with a K_d of 34 nM and B_{max} of 114 271 AFU ($n = 3$ assays, $R^2 = 0.97$). Competition binding analysis was done in which increasing concentrations of test compound were added in the presence of 90 nM **11** using HEK-293/hTLR2 cells. (B) Compound **10** has a K_i of 25 nM ($n = 5$ assays, $R^2 = 0.90$). (C) Compound **13** has a K_i of 11 nM ($n = 4$ assays, $R^2 = 0.87$).

Table 4. TLR2 Binding Affinity (K_i) Determined by Competition Binding Assays

compd	TLR2 expressing cell line	K_i (nM)	std error	R^2
10	HEK-293/hTLR2	25	1.8	0.89
10	SU.86.86	91	1.4	0.95
12	SU.86.86	25	1.7	0.90
13	HEK-293/hTLR2	11	1.8	0.87
13	SU.86.86	67	2.3	0.78

In Vivo Tumor Selectivity. Compound **13**, a conjugate with a near-infrared fluorescent dye, IRDye800CW, was used to determine in vivo TLR2 binding and selectivity for TLR2 expressing tumor xenografts (SU.86.86 cells). At 24 h after injection, in vivo fluorescence imaging detected retention of fluorescence signal in the tumor (Figure 4A). To determine the in vivo selectivity of **13** for TLR2, a blocking study was performed. A significant reduction in the tumor fluorescence was observed 24 h after injection in the blocked group that received a

dx.doi.org/10.1021/jm301002f | J. Med. Chem. 2012, 55, 9751−9762

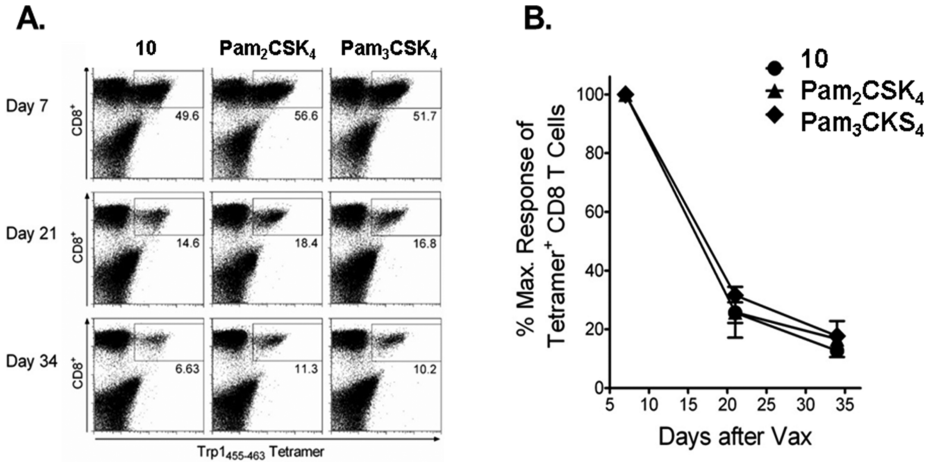

Figure 3. Evaluation of TLR2 agonists as immune adjuvants. B6 mice were immunized iv with a mixture of $Trp1_{455/9M}$ peptide, anti-CD40 monoclonal antibody, and one of the following TLR2 agonists: **10**, Pam_2CSK_4, or Pam_3CSK_4. (A) Antigen-specific CD8+ T cells in peripheral blood were measured on days 7, 21, and 34 by flow cytometry analysis of $Trp1_{455/9M}$/H-2Db tetramer staining. Numbers in each rectangular gate represent the % positive cells of all CD8+ T cells. (B) Mean maximum response of antigen-specific CD8+ T cells in peripheral blood for up to 34 days after immunization ($n = 3$). Results represent the mean and SD (error bars) of three mice per experimental group.

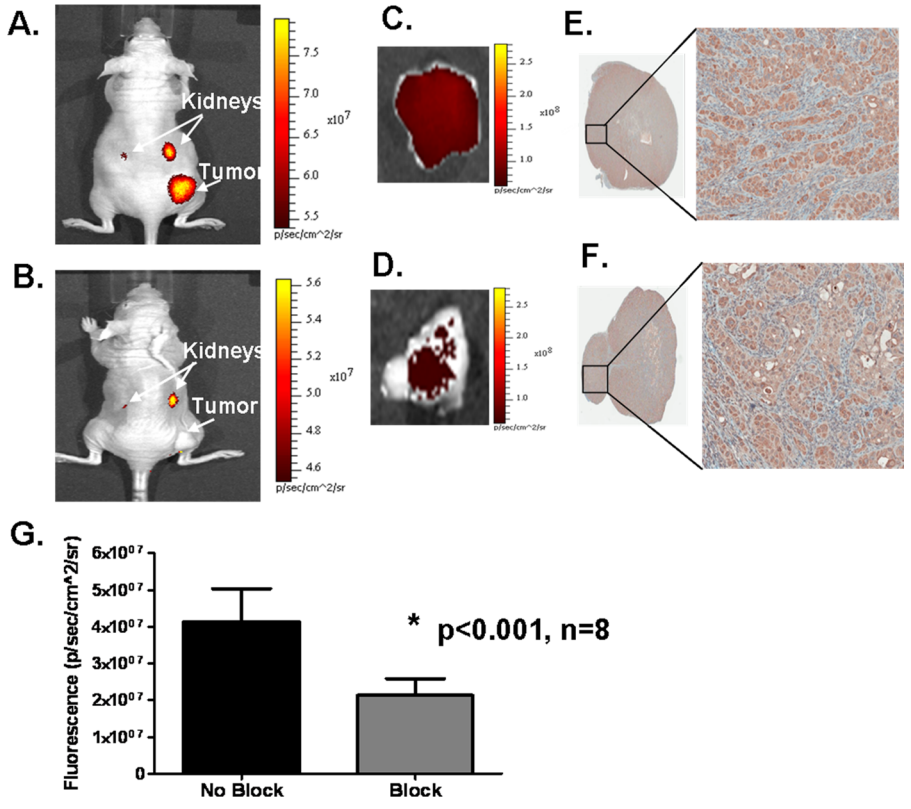

Figure 4. Comparison of representative fluorescence images of nude mice bearing TLR2 expressing tumor xenografts (SU.86.86 cells) acquired at 24 h, where the (A) unblocked mice were administered 100 nmol/kg **13** and (B) blocked mice were administered a co-injection of 100 nmol/kg **13** plus 2 μmol/kg Pam_2CSK_4 (20-fold excess). Ex vivo tumor selectivity was observed in the ex vivo fluorescence images of the unblocked and blocked tumors (C and D) and the corresponding IHC staining for TLR2 (E and F), respectively. (G) Shown are the graphed results in which a significant reduction in the in vivo fluorescence signal was measured in the blocked tumors compared to the tumors that were not blocked ($n = 8$, $p < 0.001$). The mean increase in signal (unblocked tumor/blocked tumor) of **13** in the tumor was 1.94-fold.

20-fold excess of Pam_2CSK_4 co-injected with **13** compared to the unblocked group receiving only **13** ($p < 0.001$, $n = 8$) (Figure 4A,B). The mean unblocked tumor fluorescence was 1.94-fold higher than the blocked. Ex vivo imaging confirmed that the fluorescence was associated with the tumors and that the blocked tumors had decreased fluorescence compared to the unblocked tumors (Figure 4C,D). IHC staining (Figure 4E,F) confirmed TLR2 expression in the tumors.

DISCUSSION AND CONCLUSIONS

We first investigated the SAR of a set of novel, fully synthetic compounds (**1**–**7**) through manipulation at the N-terminal

dx.doi.org/10.1021/jm301002f | J. Med. Chem. 2012, 55, 9751–9762

portion of MALP-2 derived LPs to enhance TLR2 specificity, potency, and binding affinity. Our TLR2 functional bioassay determined that these seven compounds had human TLR2 agonist activities comparable to those of the reference compounds Pam_2CSK_4 and Pam_3CSK_4. This result demonstrated that the addition of palmitoyl, fluorescein, Ac-PEGO, Ac-Aha, adapaleneyl, Ac-Aun, and tretinoyl groups on MALP-2 derived LPs did not inhibit agonist activity.

The novel TLR2 agonist analogues (**8**−**10**) of compound **3** were designed to alter the chemical properties of the parent compound in order to identify SAR that contributes to increased specificity and binding affinity. This set of compounds was derived from different origins with the goal of altering the compound properties to be more hydrophilic and soluble. Attachment of a modified CD14 peptide (**8**) or the linker Gly-DSer-PEGO-NH_2 (**10**) was found to enhance the potency, with EC_{50} values of 25 and 20 nM, respectively, compared to **3** (EC_{50} = 56 nM). The simplest and smallest compound (**10**), without inclusion of peptide, had the highest potency. Hence, the palmitoyl groups are the minimal binding/active component, and the PEGO groups or peptides serve solely to increase solubility. The IRDye800CW fluorescent dye attachment (**13**) also exhibited a potency (EC_{50} = 34 nM) similar to that of its unlabeled version (**10**), indicating that dye attachment did not significantly decrease TLR2 agonist activity. However, the addition of Eu-DTPA chelate (**11**) resulted in a 10-fold decrease in potency (EC_{50} = 204 nM). Compound **9** was synthesized by attachment of a *S. aureus* peptide to **3**, decreasing the potency (EC_{50} = 78 nM). The *S. aureus* peptide was predicted to be more acidic or at least neutral compared to SAA, with potential to improve potency. Indeed, **9** was observed to have 13-fold higher potency compared to SAA.

The SAR of novel TLR agonist compounds is typically explored using various reporter gene or functional cell-based assays.[22] In order to discover high affinity binding ligands for development of TLR2 targeted agents, we developed a lanthanide-based TRF competition binding assay. We have previously been successful in the characterization of ligand binding affinities for other receptors using this method.[23] For this purpose, compound **11** was synthesized by attachment of Eu-DTPA chelate to the potent TLR2 agonist compound **10**. Saturation binding confirmed the high TLR2 binding affinity of **11** (K_d < 100 nM), which was then used as the competing ligand in competition binding assays that confirmed the high affinities of compounds **10**, **12**, and **13** (K_i < 100 nM), which also correlated with high agonist potencies. Although **11** exhibited a 10-fold reduction in potency compared to **10**, high binding affinity was achieved.

In performing the saturation binding assays with **11**, we observed a difference in the K_d values obtained in the HEK-293/hTLR2 cell line, which was genetically engineered to highly overexpress TLR2, compared to the two human pancreatic cells lines SU.86.86 and Capan-1, which express lower endogenous levels of TLR2.[16] Similar results were also seen in the competition binding assays for both **10** and **13**, in which a reduction in binding affinity for SU.86.86 cells was observed compared to the engineered cell line. Since these TRF binding assays are performed using living cells and the ligand incubation step is longer than the time needed for receptor mediated uptake, off rates may be reduced in a receptor dependent manner and differences observed in the K_d and K_i values obtained from the different cell lines are likely due to the varying levels of TLR2 expression.

Using TLR agonists as vaccine adjuvants is a promising application that has been explored to prevent and treat cancer. We have previously reported that the use of TLR agonists as immune adjuvants in peptide vaccination together with anti-CD40 monoclonal antibodies can increase the magnitude and duration of T cell responses resulting from various types of immunizations including peptide vaccines.[10,11] Results herein show that compound **10** induced an in vivo immune response comparable to the currently available TLR2 synthetic agonists (Pam_2CSK_4 and Pam_3CSK_4), demonstrating that it can function as an immune adjuvant for use in cancer immunotherapy. Others have also reported that TLR2 agonistic LPs, based on the Pam_2CS platform, have a potential role as vaccine adjuvants.[24] It is also worth noting that no signs or symptoms of stress or toxicity were observed in the mice over the course of the study. Kimbrell et al. reported that LPs are extremely potent TLR2 agonists in vivo with no apparent toxicity in animal models.[25]

The potential use of TLR2 agonist ligands in targeted pancreatic cancer imaging and treatment was explored. We demonstrated the tumor specific retention of the fluorescently labeled compound **13**, in vivo, using mice bearing TLR2 expressing xenografts (SU.86.86 cells). Since we previously identified TLR2 as a pancreatic cancer cell surface marker expressed in over 70% of pancreatic tumors but not in normal pancreas tissue, compound **13** could potentially be used for intraoperative detection of pancreatic cancer leading to increased negative resection margins and increased pancreatic cancer survival.

EXPERIMENTAL SECTION

Compound Synthesis, Acquisition, and Preparation. Compounds were prepared as previously published by solid-phase synthesis on Rink amide Tentagel resin (0.23 mmol/g) using Fmoc/*t*Bu synthetic strategy and standard DIC-HOBt and HBTU or HCTU activations.[26] The synthesis was performed in fritted syringes using a Domino manual synthesizer obtained from Torviq (Niles, MI). For compounds **3** and **8**−**13**, an Fmoc-protected version of PEGO (Novabiochem, San Diego, CA) was used and an Fmoc protected derivative of Cys, Fmoc-Cys(*S*-[2,3-bisacyloxy-(*R*)-propyl])-OH (Fmoc-Dhc(Pam_2)-OH), was synthesized as described in Supporting Information.[27] All compounds were fully deprotected and cleaved from the resin by treatment with 91% TFA (3% water, 3% EDT, and 3% TA) or 90% TFA (5% water, 5% TIS). After ether extraction of scavengers, compounds were purified by HLPC and/or size-exclusion chromatography (Sephadex G-25, 0.1 M acetic acid) to >95% purity. All compounds were analyzed for purity by analytical HPLC and MS by ESI or MALDI-TOF (synthetic details are in Supporting Information).

Materials. N^{α}-Fmoc protected amino acids, HBTU, and HOBt were purchased from SynPep (Dublin, CA) or from Novabiochem (San Diego, CA). Rink amide Tentagel S resin was acquired from Rapp Polymere (Tubingen, Germany). HOCt, DIC, and DIEA were purchased from IRIS Biotech (Marktredwitz, Germany). The following side chain protecting groups were used for the amino acids: Arg (N^{g}-Pbf), Asn (N^{am}-Trt), Asp(*O*-*t*-Bu), Glu (*O*-*t*-Bu), His (N^{im}-Trt), Ser (*t*-Bu), DSer (*t*-Bu), Lys (N^{ε}-Boc). An Fmoc-protected version of PEGO was purchased from Novabiochem. IRDye800CW maleimide was kindly provided by LI-COR (Lincoln, NE). Adapalene was purchased from AK Scientist (aksci.com). Peptide synthesis solvents, dry solvents, and solvents for HPLC (reagent grade), and trans-retinoic acid were acquired from VWR (West Chester, PA) or Sigma-Aldrich (Milwaukee, WI) and were used without further purification unless otherwise noted. Compounds were manually assembled using 5−50 mL plastic syringe reactors equipped with a frit and a Domino manual synthesizer obtained from Torviq (Niles, MI). The C-18 Sep-Pak Vac RC cartridges for solid phase extraction were purchased from Waters (Milford, MA).

dx.doi.org/10.1021/jm301002f | J. Med. Chem. 2012, 55, 9751−9762

Peptide Synthesis. Ligands were synthesized on Tentagel Rink amide resin (initial loading, 0.2 mmol/g) using N^{α}-Fmoc protecting groups and a standard DIC/HOCt or HBTU/HOBt activation strategy. The resin was swollen in THF for an hour, washed with DMF and the Fmoc protecting group removed with 20% piperidine in DMF (2 min + 20 min). The resin was washed with DMF (3×), DCM (3×), 0.2 M HOBt in DMF (2×), and finally DMF (2×), and the first amino acid was coupled using preactivated 0.3 M HOCt ester in DMF (3 equiv of N^{α}-Fmoc amino acid, 3 equiv of HOCt, and 6 equiv of of DIC). An on-resin test using bromophenol blue was used for qualitative and continuous monitoring of reaction progress. To avoid deletion sequences and slower coupling rate in longer sequences, the double coupling was performed at all steps with 3 equiv of amino acid, 3 equiv of HBTU, and 6 equiv of DIEA in DMF. Wherever beads still tested Kaiser positive, a third coupling was performed using the symmetric anhydride method (2 equiv of amino acid and 1 equiv of DIC in dichloromethane). Any unreacted NH_2 groups on the resin thereafter were capped using an excess of 50% acetic anhydride in pyridine for 5 min. When the coupling reaction was finished, the resin was washed with DMF and the same procedure was repeated for the next amino acid until all amino acids were coupled. Fmoc-PEGO, FmocAha, Fmoc-Aun, tretinoic acid, adapalene, and fluorescein were attached to the resin as symmetrical anhydride (6 equiv of acid and 3 equiv of DIC in DCM−DMF).

Cleavage of Ligand from the Resin. A cleavage cocktail (10 mL per 1 g of resin) of TFA (91%), water (3%), triisopropylsilane (3%), and 1,2-ethylenedithiol (3%) was injected into the resin and stirred for 4 h at room temperature. Alternatively, a cleavage cocktail of 90% trifluoroacetic acid (5% water and 5% triisopropylsilane) was used. The crude ligand was isolated from the resin by filtration. The filtrate was reduced to low volume by evaporation using a stream of nitrogen, and the ligand was precipitated in ice-cold diethyl ether, washed several times with ether, dried, dissolved in water, and lyophilized to give off-white solid powders that were stored at −20 °C until purified. The crude compound was purified by size-exclusion chromatography.

Synthesis of Compound 11, Eu-DTPA Labeled Compound. Attachment of DTPA to the N-terminus of was performed using preformed HOBt activation (3 equiv of DTPA anhydride and 6 equiv of HOBt, Scheme 1). DTPA was attached to H-PEGO-Dhc(Pam_2)-Gly-DSer-PEGO resin as follows. Briefly, DTPA anhydride (3 equiv) and HOBt (6 equiv) in DMSO were heated until they were dissolved (60 °C). Then the mixture was stirred for 30 min at room temperature. The preformed DTPA-OBt diester was injected into the free-amine H-PEGO-Dhc(Pam_2)-Gly-DSer-PEGO resin and stirred overnight. The resin was washed with DMSO, THF, 5% DIEA 5% water in THF (5 min), THF, and DCM. The compound was cleaved from the resin as described above and purified by HPLC. The purified peptide was dissolved in 0.1 M ammonium acetate buffer, pH 8.0. Then 3.0 equiv of $Eu(III)Cl_3$ was added and the mixture was stirred at room temperature overnight. The Eu-labeled peptide was separated using solid-phase extraction (SPE) and lyophilized to yield an amorphous white powder. The final compound was characterized by HPLC (TEAA buffer, pH 6.0), ESI-MS, and/or FT-ICR.

Synthesis of Compounds 12 and 13. Attachment of Trt-Mpr-OH (*S*-trityl-3-mercaptopropionic acid) to the N-terminus H-PEGO-Dhc(Pam_2)-Gly-DSer-PEGO-resin was performed using preformed HBTU activation (3 equiv of Trt-Mpr-OH, 3 equiv of HBTU, and 6 equiv of DIEA in DMF) (Scheme 1). The resin was washed with DMF and DCM. Compound **12** was cleaved from the resin as described above and purified by HPLC.

Compound **12**, H-Mpr-PEGO-Dhc(Pam_2)-Gly-DSer-PEGO-NH_2 (1 μmol), was dissolved in 1 mL of DMF and reacted with 1 equiv of IRDye800CW maleimide under argon atmosphere. The reaction was monitored by HPLC and additional aliquots (0.1 equiv) of dye were added until the reaction was complete. The compound was purified by HPLC. The conjugate, compound **13** (IRDye800CW-Mpr-PEGO-Dhc(Pam_2)-Gly-DSer-PEGO-NH_2), was purified by HPLC.

Purification and Analysis. Purity of the peptides was ensured using analytical HPLC (Waters Alliance 2695 separation model with a dual wavelength detector Waters 2487) with a reverse-phase column (Waters Symmetry, 3.0 mm × 75 mm, 3.5 μm; flow rate of 0.3 mL/min). HPLC conditions were as follows: HPLC, pH 2, linear gradient from 10% to 90% B over 30 min, where A is 0.1% TFA and B is acetonitrile or THF; HPLC pH 6, linear gradient from 10% to 90% B over 30 min, where A is 0.1% TEAA and B is acetonitrile or THF. Size exclusion chromatography was performed on a borosilicate glass column (2.6 mm × 250 mm, Sigma, St. Louis, MO) filled with medium sized Sephadex G-25 or G-10. The compounds were eluted with an isocratic flow of 1.0 M aqueous acetic acid.

Solid-phase extraction was employed where simple isolation of final compound was needed from excess salts and buffers, e.g., for lanthaligand synthesis. For this purpose, C-18 Sep-Pak cartridges (100 or 500 mg) were used and preconditioned initially with 5 column volumes (5 times the volume of packed column bed) each of acetonitrile, methanol, and water, in that order. After the compound was loaded, the column was washed several times with water and then gradually with 5%, 10%, 20%, 30%, 50%, and 70% of aqueous acetonitrile to elute the peptide. Structures were characterized by ESI (Finnigan, Thermoquest LCQ ion trap instrument), MALDI-TOF, or FT-ICR mass spectrometry. An appropriate mixture of standard peptides was used for internal calibrations.

The test compounds (**1**−**13**) were dissolved in DMSO at 1 mg/mL as stock solutions stored at −20 °C. For biological experimental use, 10 μg/mL working solutions of the compounds were prepared from stock solutions in sterilized, deionized water and used immediately.

Acquisition of Commercially Available Compounds and Antibodies. Commercially available synthetic TLR2 agonists were used as references. Pam_2CSK_4 and Pam_3CSK_4 were purchased from InvivoGen (San Diego, CA), and recombinant human apo-SAA1 was purchased from PeproTech (Rocky Hill, NJ).

$Trp1_{455/9M}$ (TAPDNLGYM) is an H-$2D^b$-optimized peptide for MHC class I binding[28] and was obtained from A&A Labs (San Diego, CA). Rat anti-mouse CD40 monoclonal antibody was prepared from the FGK45.5 hybridoma culture supernatants.[11] FITC-conjugated anti-MHC class II and PerCP Cy5.5-conjugated CD8a antibodies were both purchased from eBioscience (San Diego, CA). Phycoerythrin-conjugated $Trp1_{455/9M}$/H-$2D^b$ tetramers were provided by the NIH Tetramer Facility, Emory University (Atlanta, GA).

Cell Culture. The parental HEK-293 cells (ATCC CRL-1573) and Capan-I cells (ATCC HTB-79) were cultured in DMEM/F12 medium (Life Technologies Gibco) supplemented with 10% normal calf serum (NCS) (Atlanta Biologicals, Lawrenceville, GA) and 1% penicillin/streptomycin solution (Sigma). The HEK-293/hTLR2 cells (InvivoGen, San Diego, CA) were cultured in DMEM/F12 medium supplemented with 10% NCS, 1% penicillin/streptomycin solution, 10 μg/mL blasticidin (InvivoGen). The SU.86.86 cells (ATCC CRL-1837) were grown in RPMI 1640 medium (Life Technologies Gibco) supplemented with 10% NCS. All cells were grown at 37 °C and 5% CO_2.

The HEK-293/hTLR2 cells were genetically engineered to highly overexpress TLR2 by stable transfection of the parental HEK-293 cells with pUNO-hTLR2 plasmid expressing the human TLR2 gene.[29] The expression of human TLR2 in HEK-293/hTLR2 cells and absence in the parental HEK-293 cells were confirmed by RT-PCR and Western blot analysis (Supporting Information Figure 1A,B). The two human pancreatic cells lines used in our studies, SU.86.86 and Capan-I, express endogenous levels of TLR2.[16]

In Vitro TLR2 Functional Bioassay. The in vitro TLR2 functional bioassay was developed and optimized for use in high-throughput screening of soluble compound libraries to identify both TLR2 agonists and antagonists. The bioassay measures the induction of NF-κB signaling via TLR2 in HEK-293/hTLR2 cells and parental HEK-293 cells as a negative control. Cells were seeded at a density of 40 000 per well using a WellMate microplate dispenser (Thermo Fisher Scientific/Matrix) in black 96-well plates with opaque white wells (PerkinElmer, Waltham, MA) and then incubated at 37 °C. On day 2, the cells were transiently transfected with pNifty-Luc(InvivoGen, San Diego, CA), an NF-κB inducible reporter plasmid expressing the luciferase reporter gene[29] using an optimized 4:1 ratio by volume of FugeneHD transfection reagent (Promega, Madison, WI) to pNifty-Luc plasmid DNA (1 μg/mL). On day 3, the cells were stimulated with either test

peptides or controls adjusted to a final concentration of 1 μg/mL using a NanoDrop spectrophotometer, ND1000 (Thermo Fisher Scientific). Synthetic di- and triacylated LP ligands, Pam_2CSK_4 and Pam_3CSK_4 (InvivoGen), were used as positive controls. TNF-α (InvivoGen) was also used as a transfection control that induces NF-κB independently of TLR2. On day 4 after 24 h of peptide stimulation, luciferase induced activity by the induction of NF-κB was measured. The medium was aspirated from the wells using an ELx405 SelectCW plate washer (BioTek, Winooski, VT), and 150 μg/mL D-luciferin (Gold Biotechnology, St. Louis, MO) was dispensed using the microplate dispensor. The plates were incubated at 37 °C for 5 min. The luminescence intensity was measured using the standard luminescence protocol on a Victor X4 multilabel plate reader equipped with a plate stacker for readout of multiple plates at a time (PerkinElmer, Waltham, MA). For each in vitro TLR2 bioassay, at least three different experiments were performed in triplicate ($n \geq 3$). Data were analyzed with GraphPad Prism software, and curves were generated with the appropriate nonlinear fit regression analysis.

In Cyto Europium Time-Resolved Fluorescence Binding Assays. Europium TRF binding assays were performed as previously described with slight modifications using three cell lines that express TLR2: HEK-293/hTLR2, SU.86.86, and Capan-I.[23a,d,30] The Capan-I and SU.86.86 cells were plated in 96-well black plates with white opaque wells (PerkinElmer), while the HEK-293/hTLR2 cells were plated on 96-well poly-D-lysine coated plates (Sigma-Aldrich) to aid in the attachment of these cells to the plate. Cells were grown in the 96-well plates for 2 days, reaching approximately 80% confluency. Both types of plates were evaluated for nonspecific binding and background signal.

For saturation binding, increased concentrations of the labeled ligand, compound **11** (Table 3), were used to determine total binding to TLR2. Nonspecific binding was determined in the presence of 1 μM Pam_2CSK_4. On the day of the experiment the medium was aspirated. Then 50 μL of binding buffer was added to the total binding wells and 50 μL of Pam_2CSK_4 was added to the nonspecific wells and then allowed to incubate for 30 min at 37 °C. Next, an amount of 50 μL of the serial dilutions of **10** was added and then allowed to incubate for 1 h at 37 °C. Cells were washed three times to remove unbound ligand. Next, 100 μL of DELFIA enhancement solution (PerkinElmer) was added to each well. Cells were incubated for 30 min at 37 °C prior to reading. The plates were read on the VICTOR X4 multilabel plate reader using the standard europium TRF protocol (340 nm excitation, 400 μs delay, and 400 μs emission collection at 615 nm). To determine the mean K_d, statistical analysis was performed using GraphPad Prism software.

Competition binding assays were performed to test the TLR2 binding specificity of the test ligands using two cell lines: HEK-293/hTLR2 and SU.86.86. Cells were grown in 96-well plates for 2 days, reaching approximately 80% confluency. On the day of the experiment, the cell culture medium was aspirated and 50 μL of nonlabeled test ligand was added in a series of decreasing concentrations (1 μM to 0.01 nM) followed by 50 μL of the competing Eu-labeled ligand **10** at a fixed concentration of 90 nM. Cells were incubated with labeled and unlabeled ligands for 1 h at 37 °C. Following incubation, cells were washed three times to remove unbound ligand. Next, 100 μL of DELFIA enhancement solution (PerkinElmer) was added to each well. Cells were incubated for 30 min at 37 °C prior to reading. The plates were read on a PerkinElmer VICTOR X4 multilabel reader using the standard europium TRF protocol. To determine the mean K_i, statistical analysis was performed using GraphPad Prism software.

Animal Studies. All procedures were in compliance with the Guide for the Care and Use of Laboratory Animal Resources (1996), National Research Council, and approved by the Institutional Animal Care and Use Committee, University of South Florida. Mice are housed in a clean facility with special conditions that include HEPA filtered ventilated cage systems, autoclaved bedding, autoclaved housing, autoclaved water, irradiated food, and special cage changing procedures. Mice are handled under aseptic conditions including the wearing of gloves, gowns, and shoe coverings.

In Vivo Cellular Immune Response Assays. To assess the efficacy of **10** as an immune adjuvant, we tested it in our previously reported optimized peptide vaccine, TriVax, comprising synthetic peptides, TLR agonists, and anti-CD40 antibodies.[11] The 6−8 week old C57BL/6 (B6) mice (Charles River,Wilmington, MA) were immunized iv with a mixture (in a volume of 200 μL) of 100 μg of optimized $Trp1_{455/9M}$ peptide,[28] 50 μg of anti-CD40 monoclonal antibody (Clone, FGk-45.5),[11] and 50 μg of TLR2 agonist (**10**, Pam_2CSK_4, or Pam_3CSK_4). The $Trp1_{455/9M}$ peptide (TAPDNLGYM) is a heterocyclic analogue of the tyrosinase-related protein-1 (Trp1) sequence.[28] $Trp1_{455/9M}$ is presented to CD8+ T cells via the H-$2D^b$ MHC I molecules to elicit an immune response.[28] $Trp1_{455/9M}$ has increased biostability and enhanced CD8+ T cell response with no CD4+ T cell response for an improved immune induction in the TriVax vaccine.[6a] The cellular immune response of $Trp1_{455/9M}$/ H-$2D^b$ tetramer positive CD8+ T cells in the blood was measured on days 7, 21, and 34. Cellular immune responses were analyzed by tetramer staining, in which tetramers, comprising synthetic tetrameric MHC class I peptide complexes, are used to stain antigen-specific T cells by FACS analysis.[6b,31] For tetramer staining, peripheral blood was taken from the submandibular vein and treated briefly with ammonium chloride buffer to lyse red blood cells. Blood cells were stained for 40 min on ice with PerCP Cy5.5-conjugated CD8a antibody to determine CD8+ T cell expression, phycoerythrin-conjugated $Trp1_{455/9M}$/H-$2D^b$ tetramers for identification of MHC I presentation of $Trp1_{455/9M}$/H-$2D^b$, and FITC-conjugated anti-MHC class II antibody as a control for nonspecific binding of the tetramers by MHC II positive cells, e.g., macrophages. Fluorescence was evaluated using a FACSCalibur flow cytometer (BD Biosciences). Tetramer positive CD8+ T cells identified by gating and analyses were performed using FlowJo software. Fluorescence was evaluated using a FACSCalibur flow cytometer (BD Biosciences). $Trp1_{455/9M}$/H-$2D^b$ tetramer positive CD8+ T cells were identified by gating, and analyses were performed using FlowJo software.

In Vivo TLR2 Selectivity Experiment. Female athymic nude mice 6−8 weeks old (Harlan) bearing human pancreatic tumor xenografts consisting of SU.86.86 cells on the right flank were used for this study. Mouse weights and tumor volumes were determined using caliper measurements and the formula volume (mm^3) = (length × $width^2$)/2. Images were acquired when the tumors reached an average size of 500 mm^3. For the blocked group, a co-injection of 100 nmol/kg of the fluorescently labeled compound **13** plus 2 μmol/kg Pam_2CSK_4 (a 20-fold excess) was administered via tail vein injection. For the unblocked group, 100 nmol/kg **13** was administered. Fluorescence images were acquired at 0 and 24 h using the Caliper Xenogen IVIS200 system (PerkinElmer) with the 710−760 nm excitation and 810−875 nm emission filter set. The fluorescence was quantified using Living Image software, in which the quantified signals were corrected for both instrument and mouse background subtractions. The quantified fluorescence was then plotted using GraphPad Prism software and underwent statistical analysis using Student's t test.

For further confirmation of ligand **13** specificity for TLR2, ex vivo fluorescence imaging and histological analyses were performed on the tumors. For histological analyses the samples were fixed in 10% formalin solution, processed, embedded, sectioned, and either H&E stained for the presence of tumor or underwent IHC staining using TLR2 antibody (Abcam no. ab24192).

Statistical Analysis. The results are represented as mean ± SD and statistically evaluated by Student's t test to determine statistical significance.

■ ASSOCIATED CONTENT

Ⓢ Supporting Information

Complete information on general methods and synthesis, solid phase synthesis QC and purification, mass spectrometry, TLR2 functional bioassay validation and optimization, dose−response curves, saturation binding analysis, and competition binding analysis. This material is available free of charge via the Internet at http://pubs.acs.org.

AUTHOR INFORMATION

Corresponding Author

*For D.L.M.: phone, 813-745-8948; fax, 813-745-8357; e-mail, david.morse@moffitt.org. For J.V.: phone, 520-626-4179; fax, 520-626-4824; e-mail, vagner@email.arizona.edu.

Notes

The authors declare no competing financial interest.

ACKNOWLEDGMENTS

The authors thank the staff of the Moffitt Small Animal Modeling and Imaging Shared Resource, Tissue Core, Analytic Microscopy Core, and Comparative Biomedicine for their technical support. We also thank Michael Olive and LI-COR Biosciences for providing NIR dye. This work was supported by the NIH Grants R01-CA123547, R01-CA103921, and R01-CA136828.

ABBREVIATIONS USED

Boc, *tert*-butyloxycarbonyl; BB, bromophenol blue; *t*-Bu, *tert*-butyl; CH_3CN, acetonitrile; DCM, dichloromethane; DI, deionized; DIPEA, diisopropylethylamine; Dhc, 2,3-dihydroxypropylcysteine or Cys(*S*-[2,3-hydroxy-(*R*)-propyl] residue; DMF, *N*,*N*-dimethylformamide; DIC, diisopropylcarbodiimide; DMEM, Dulbecco's modified Eagle medium; Eu-DTPA, europium diethylenetriaminepentaacetic acid; Fmoc, 9-fluorenylmethoxycarbonyl; FT-ICR, Fourier transform ion cyclotron resonance; ESI-MS, electrospray ionization mass spectrometry; EDT, 1,2-ethanedithiol; Et_2O, diethyl ether; HBSS, Hank's balanced saline solution buffered with 25 mM Hepes; HCTU, *O*-[1*H*-6-chlorobenzotriazol-1-yl)(dimethylamino)ethylene]-uronium hexafluorophosphate *N*-oxide; HEPES, 4-(2-hydroxyethyl)-1-piperazineethanesulfonic acid; HOBt, *N*-hydroxybenzotriazole; HOCt, 6-chloro-1-hydroxybenzotriazole; LP, lipopeptide; MALDI-TOF, matrix assisted laser desorption ionization time of flight; MALP-2, macrophage-activating lipopeptide 2; Mpr, 3-mercaptopropionic residue; PAMP, pathogen-associated molecular pattern; Pbf, 2,2,4,6,7-pentamethyl-dihydrobenzofuran-5-sulfonyl; PEGO, 19-amino-5-oxo-3,10,13,16-tetraoxo-6-azanonadecan-1-oic acid residue; PRR, pattern recognition receptor; SPPS, solid-phase peptide synthesis; RP-HPLC, reverse-phase high performance liquid chromatography; SAA, serum amyloid A; SAR, structure–activity relationship; TA, thioanisole; THF, tetrahydrofuran; TIR, Toll/interleukin receptor; TIS, triisopropylsilane; TFA, trifluoroacetic acid; TLR2, Toll-like receptor 2; TNF-α, tumor necrosis factor α; TRF, time-resolved fluorescence; Trt, trityl

ADDITIONAL NOTE

Abbreviations used for amino acids and designation of peptides follow the rules of the IUPAC-IUB Commission of Biochemical Nomenclature in *J. Biol. Chem.* **1972**, *247*, 977–983.

REFERENCES

(1) (a) Cheng, N.; He, R.; Tian, J.; Ye, P. P.; Ye, R. D. Cutting edge: TLR2 is a functional receptor for acute-phase serum amyloid A. *J. Immunol.* **2008**, *181* (1), 22–26. (b) Kanzler, H.; Barrat, F. J.; Hessel, E. M.; Coffman, R. L. Therapeutic targeting of innate immunity with Toll-like receptor agonists and antagonists. *Nat. Med.* **2007**, *13* (5), 552–559. (c) Zuany-Amorim, C.; Hastewell, J.; Walker, C. Toll-like receptors as potential therapeutic targets for multiple diseases. *Nat. Rev. Drug Discovery* **2002**, *1* (10), 797–807.

(2) (a) Jarnicki, A. G.; Conroy, H.; Brereton, C.; Donnelly, G.; Toomey, D.; Walsh, K.; Sweeney, C.; Leavy, O.; Fletcher, J.; Lavelle, E. C.; Dunne, P.; Mills, K. H. Attenuating regulatory T cell induction by TLR agonists through inhibition of p38 MAPK signaling in dendritic cells enhances their efficacy as vaccine adjuvants and cancer immunotherapeutics. *J. Immunol.* **2008**, *180* (6), 3797–3806. (b) Marshall, N. A.; Galvin, K. C.; Corcoran, A. M.; Boon, L.; Higgs, R.; Mills, K. H. Immunotherapy with PI3K inhibitor and Toll-like receptor agonist induces IFN-gamma+IL-17+polyfunctional T cells that mediate rejection of murine tumors. *Cancer Res.* **2012**, *72* (3), 581–591. (c) Adams, S. Toll-like receptor agonists in cancer therapy. *Immunotherapy* **2009**, *1* (6), 949–964.

(3) (a) Akira, S.; Takeda, K. Toll-like receptor signalling. *Nat. Rev. Immunol.* **2004**, *4* (7), 499–511. (b) West, A. P.; Koblansky, A. A.; Ghosh, S. Recognition and signaling by Toll-like receptors. *Annu. Rev. Cell Dev. Biol.* **2006**, *22*, 409–437.

(4) (a) Jin, M. S.; Lee, J. O. Structures of the Toll-like receptor family and its ligand complexes. *Immunity* **2008**, *29* (2), 182–191. (b) Ozinsky, A.; Underhill, D. M.; Fontenot, J. D.; Hajjar, A. M.; Smith, K. D.; Wilson, C. B.; Schroeder, L.; Aderem, A. The repertoire for pattern recognition of pathogens by the innate immune system is defined by cooperation between Toll-like receptors. *Proc. Natl. Acad. Sci. U.S.A.* **2000**, *97* (25), 13766–13771.

(5) (a) Janeway, C. A., Jr.; Medzhitov, R. Innate immune recognition. *Annu. Rev. Immunol.* **2002**, *20*, 197–216. (b) Akira, S.; Takeda, K.; Kaisho, T. Toll-like receptors: critical proteins linking innate and acquired immunity. *Nat. Immunol.* **2001**, *2* (8), 675–680. (c) Kawai, T.; Akira, S. The role of pattern-recognition receptors in innate immunity: update on Toll-like receptors. *Nat. Immunol.* **2010**, *11* (5), 373–384.

(6) (a) Cho, H. I.; Lee, Y. R.; Celis, E. Interferon gamma limits the effectiveness of melanoma peptide vaccines. *Blood* **2011**, *117* (1), 135–144. (b) Serbina, N.; Pamer, E. G. Quantitative studies of CD8+ T-cell responses during microbial infection. *Curr. Opin. Immunol.* **2003**, *15* (4), 436–442. (c) Ingale, S.; Wolfert, M. A.; Buskas, T.; Boons, G. J. Increasing the antigenicity of synthetic tumor-associated carbohydrate antigens by targeting Toll-like receptors. *ChemBioChem* **2009**, *10* (3), 455–463. (d) Buskas, T.; Thompson, P.; Boons, G. J. Immunotherapy for cancer: synthetic carbohydrate-based vaccines. *Chem. Commun.* **2009**, *36*, 5335–5349.

(7) Hennessy, E. J.; Parker, A. E.; O'Neill, L. A. Targeting Toll-like receptors: emerging therapeutics? *Nat. Rev. Drug Discovery* **2010**, *9* (4), 293–307.

(8) (a) Simons, M. P.; O'Donnell, M. A.; Griffith, T. S. Role of neutrophils in BCG immunotherapy for bladder cancer. *Urol. Oncol.* **2008**, *26* (4), 341–345. (b) Murata, M. Activation of Toll-like receptor 2 by a novel preparation of cell wall skeleton from *Mycobacterium bovis* BCG Tokyo (SMP-105) sufficiently enhances immune responses against tumors. *Cancer Sci.* **2008**, *99* (7), 1435–1440.

(9) Schmidt, J.; Welsch, T.; Jager, D.; Muhlradt, P. F.; Buchler, M. W.; Marten, A. Intratumoural injection of the Toll-like receptor-2/6 agonist "macrophage-activating lipopeptide-2" in patients with pancreatic carcinoma: a phase I/II trial. *Br. J. Cancer* **2007**, *97* (5), 598–604.

(10) Celis, E. Toll-like receptor ligands energize peptide vaccines through multiple paths. *Cancer Res.* **2007**, *67* (17), 7945–7947.

(11) Cho, H. I.; Celis, E. Optimized peptide vaccines eliciting extensive CD8 T-cell responses with therapeutic antitumor effects. *Cancer Res.* **2009**, *69* (23), 9012–9009.

(12) *Cancer Facts & Figures—2012*; American Cancer Society: Atlanta, GA, 2012; pp 1–63.

(13) (a) Ferrone, C. R.; Brennan, M. F.; Gonen, M.; Coit, D. G.; Fong, Y.; Chung, S.; Tang, L.; Klimstra, D.; Allen, P. J. Pancreatic adenocarcinoma: the actual 5-year survivors. *J. Gastrointest. Surg.* **2008**, *12* (4), 701–706. (b) Howard, T. J.; Krug, J. E.; Yu, J.; Zyromski, N. J.; Schmidt, C. M.; Jacobson, L. E.; Madura, J. A.; Wiebke, E. A.; Lillemoe, K. D. A margin-negative R0 resection accomplished with minimal postoperative complications is the surgeon's contribution to long-term survival in pancreatic cancer. *J. Gastrointest. Surg.* **2006**, *10* (10), 1338–1345.

(14) (a) Angst, E.; Kim-Fuchs, C.; Chittazhathu Kurian Kuruvilla, Y.; Inderbitzin, D.; Montani, M.; Candinas, D.; Gloor, B. How to counter the problem of r1 resection in duodenopancreatectomy for pancreatic cancer? *J. Gastrointest. Surg.* **2012**, *16* (3), 673. (b) Esposito, I.; Kleeff, J.;

Bergmann, F.; Reiser, C.; Herpel, E.; Friess, H.; Schirmacher, P.; Buchler, M. W. Most pancreatic cancer resections are R1 resections. *Ann. Surg. Oncol.* **2008**, *15* (6), 1651−1660. (c) Campbell, F.; Smith, R. A.; Whelan, P.; Sutton, R.; Raraty, M.; Neoptolemos, J. P.; Ghaneh, P. Classification of R1 resections for pancreatic cancer: the prognostic relevance of tumour involvement within 1 mm of a resection margin. *Histopathology* **2009**, *55* (3), 277−283.

(15) (a) van Dam, G. M.; Themelis, G.; Crane, L. M.; Harlaar, N. J.; Pleijhuis, R. G.; Kelder, W.; Sarantopoulos, A.; de Jong, J. S.; Arts, H. J.; van der Zee, A. G.; Bart, J.; Low, P. S.; Ntziachristos, V. Intraoperative tumor-specific fluorescence imaging in ovarian cancer by folate receptor-alpha targeting: first in-human results. *Nat. Med.* **2011**, *17* (10), 1315−1319. (b) Sevick-Muraca, E. M.; Sharma, R.; Rasmussen, J. C.; Marshall, M. V.; Wendt, J. A.; Pham, H. Q.; Bonefas, E.; Houston, J. P.; Sampath, L.; Adams, K. E.; Blanchard, D. K.; Fisher, R. E.; Chiang, S. B.; Elledge, R.; Mawad, M. E. Imaging of lymph flow in breast cancer patients after microdose administration of a near-infrared fluorophore: feasibility study. *Radiology* **2008**, *246* (3), 734−741. (c) Tagaya, N.; Yamazaki, R.; Nakagawa, A.; Abe, A.; Hamada, K.; Kubota, K.; Oyama, T. Intraoperative identification of sentinel lymph nodes by near-infrared fluorescence imaging in patients with breast cancer. *Am. J. Surg.* **2008**, *195* (6), 850−853. (d) Stummer, W.; Pichlmeier, U.; Meinel, T.; Wiestler, O. D.; Zanella, F.; Reulen, H. J. Fluorescence-guided surgery with 5-aminolevulinic acid for resection of malignant glioma: a randomised controlled multicentre phase III trial. *Lancet Oncol.* **2006**, *7* (5), 392−401. (e) Hadjipanayis, C. G.; Jiang, H.; Roberts, D. W.; Yang, L. Current and future clinical applications for optical imaging of cancer: from intraoperative surgical guidance to cancer screening. *Semin. Oncol.* **2011**, *38* (1), 109−118. (f) Keereweer, S.; Hutteman, M.; Kerrebijn, J. D.; van de Velde, C. J.; Vahrmeijer, A. L.; Lowik, C. W. Translational optical imaging in diagnosis and treatment of cancer. *Curr. Pharm. Biotechnol.* **2012**, *13* (4), 498−503. (g) Ntziachristos, V.; Yoo, J. S.; van Dam, G. M. Current concepts and future perspectives on surgical optical imaging in cancer. *J. Biomed. Opt.* **2010**, *15* (6), 066024. (h) Nguyen, Q. T.; Olson, E. S.; Aguilera, T. A.; Jiang, T.; Scadeng, M.; Ellies, L. G.; Tsien, R. Y. Surgery with molecular fluorescence imaging using activatable cell-penetrating peptides decreases residual cancer and improves survival. *Proc. Natl. Acad. Sci. U.S.A.* **2010**, *107* (9), 4317−4322.

(16) Morse, D. L.; Balagurunathan, Y.; Hostetter, G.; Trissal, M.; Tafreshi, N. K.; Burke, N.; Lloyd, M.; Enkemann, S.; Coppola, D.; Hruby, V. J.; Gillies, R. J.; Han, H. Identification of novel pancreatic adenocarcinoma cell-surface targets by gene expression profiling and tissue microarray. *Biochem. Pharmacol.* **2012**, *80* (5), 748−754.

(17) (a) Muhlradt, P. F.; Kiess, M.; Meyer, H.; Sussmuth, R.; Jung, G. Isolation, structure elucidation, and synthesis of a macrophage stimulatory lipopeptide from *Mycoplasma fermentans* acting at picomolar concentration. *J. Exp. Med.* **1997**, *185* (11), 1951−1958. (b) Muhlradt, P. F.; Kiess, M.; Meyer, H.; Sussmuth, R.; Jung, G. Structure and specific activity of macrophage-stimulating lipopeptides from *Mycoplasma hyorhinis*. *Infect. Immun.* **1998**, *66* (10), 4804−4810. (c) Takeuchi, O.; Kawai, T.; Muhlradt, P. F.; Morr, M.; Radolf, J. D.; Zychlinsky, A.; Takeda, K.; Akira, S. Discrimination of bacterial lipoproteins by Toll-like receptor 6. *Int. Immunol.* **2001**, *13* (7), 933−940.

(18) (a) Alexopoulou, L.; Thomas, V.; Schnare, M.; Lobet, Y.; Anguita, J.; Schoen, R. T.; Medzhitov, R.; Fikrig, E.; Flavell, R. A. Hyporesponsiveness to vaccination with *Borrelia burgdorferi* OspA in humans and in TLR1- and TLR2-deficient mice. *Nat. Med.* **2002**, *8* (8), 878−884. (b) Morr, M.; Takeuchi, O.; Akira, S.; Simon, M. M.; Muhlradt, P. F. Differential recognition of structural details of bacterial lipopeptides by Toll-like receptors. *Eur. J. Immunol.* **2002**, *32* (12), 3337−3347. (c) Takeuchi, O.; Sato, S.; Horiuchi, T.; Hoshino, K.; Takeda, K.; Dong, Z.; Modlin, R. L.; Akira, S. Cutting edge: role of Toll-like receptor 1 in mediating immune response to microbial lipoproteins. *J. Immunol.* **2002**, *169* (1), 10−14. (d) Jin, M. S.; Kim, S. E.; Heo, J. Y.; Lee, M. E.; Kim, H. M.; Paik, S. G.; Lee, H.; Lee, J. O. Crystal structure of the TLR1-TLR2 heterodimer induced by binding of a tri-acylated lipopeptide. *Cell* **2007**, *130* (6), 1071−1082. (e) Manavalan, B.; Basith, S.; Choi, S. Similar structures but different roles—an updated perspective on TLR structures. *Front. Physiol.* **2011**, *2*, 41. (f) Kang, J. Y.; Nan, X.; Jin, M. S.; Youn, S. J.; Ryu, Y. H.; Mah, S.; Han, S. H.; Lee, H.; Paik, S. G.; Lee, J. O. Recognition of lipopeptide patterns by Toll-like receptor 2-Toll-like receptor 6 heterodimer. *Immunity* **2009**, *31* (6), 873−884. (g) Buwitt-Beckmann, U.; Heine, H.; Wiesmuller, K. H.; Jung, G.; Brock, R.; Ulmer, A. J. Lipopeptide structure determines TLR2 dependent cell activation level. *FEBS J.* **2005**, *272* (24), 6354−6364. (h) Yamamoto, M.; Takeda, K. Current views of Toll-like receptor signaling pathways. *Gastroenterol. Res. Pract.* **2010**, 240365.

(19) Uhlar, C. M.; Whitehead, A. S. Serum amyloid A, the major vertebrate acute-phase reactant. *Eur. J. Biochem.* **1999**, *265* (2), 501−523.

(20) Manukyan, M.; Triantafilou, K.; Triantafilou, M.; Mackie, A.; Nilsen, N.; Espevik, T.; Wiesmuller, K. H.; Ulmer, A. J.; Heine, H. Binding of lipopeptide to CD14 induces physical proximity of CD14, TLR2 and TLR1. *Eur. J. Immunol.* **2005**, *35* (3), 911−921.

(21) Fujimoto, Y.; Hashimoto, M.; Furuyashiki, M.; Katsumoto, M.; Seya, T.; Suda, Y.; Fukase, K. Lipopeptides from *Staphylococcus aureus* as Tlr2 ligands: prediction with mRNA expression, chemical synthesis, and immunostimulatory activities. *ChemBioChem* **2009**, *10* (14), 2311−2315.

(22) Czarniecki, M. Small molecule modulators of Toll-like receptors. *J. Med. Chem.* **2008**, *51* (21), 6621−6626.

(23) (a) Handl, H. L.; Vagner, J.; Yamamura, H. I.; Hruby, V. J.; Gillies, R. J. Development of a lanthanide-based assay for detection of receptor-ligand interactions at the delta-opioid receptor. *Anal. Biochem.* **2005**, *343* (2), 299−307. (b) Xu, L.; Vagner, J.; Josan, J.; Lynch, R. M.; Morse, D. L.; Baggett, B.; Han, H.; Mash, E. A.; Hruby, V. J.; Gillies, R. J. Enhanced targeting with heterobivalent ligands. *Mol. Cancer Ther.* **2009**, *8* (8), 2356−2365. (c) Barkey, N. M.; Tafreshi, N. K.; Josan, J. S.; De Silva, C. R.; Sill, K. N.; Hruby, V. J.; Gillies, R. J.; Morse, D. L.; Vagner, J. Development of melanoma-targeted polymer micelles by conjugation of a melanocortin 1 receptor (MC1R) specific ligand. *J. Med. Chem.* **2011**, *54* (23), 8078−8084. (d) Josan, J. S.; Morse, D. L.; Xu, L.; Trissal, M.; Baggett, B.; Davis, P.; Vagner, J.; Gillies, R. J.; Hruby, V. J. Solid-phase synthetic strategy and bioevaluation of a labeled delta-opioid receptor ligand Dmt-Tic-Lys for in vivo imaging. *Org. Lett.* **2009**, *11* (12), 2479−2482.

(24) (a) Agnihotri, G.; Crall, B. M.; Lewis, T. C.; Day, T. P.; Balakrishna, R.; Warshakoon, H. J.; Malladi, S. S.; David, S. A. Structure−activity relationships in Toll-like receptor 2-agonists leading to simplified monoacyl lipopeptides. *J. Med. Chem.* **2011**, *54* (23), 8148−8160. (b) Salunke, D. B.; Shukla, N. M.; Yoo, E.; Crall, B. M.; Balakrishna, R.; Malladi, S. S.; David, S. A. Structure−activity relationships in human Toll-like receptor 2-specific monoacyl lipopeptides. *J. Med. Chem.* **2012**, *55* (7), 3353−3363.

(25) Kimbrell, M. R.; Warshakoon, H.; Cromer, J. R.; Malladi, S.; Hood, J. D.; Balakrishna, R.; Scholdberg, T. A.; David, S. A. Comparison of the immunostimulatory and proinflammatory activities of candidate Gram-positive endotoxins, lipoteichoic acid, peptidoglycan, and lipopeptides, in murine and human cells. *Immunol. Lett.* **2008**, *118* (2), 132−141.

(26) (a) Vagner, J.; Xu, L.; Handl, H. L.; Josan, J. S.; Morse, D. L.; Mash, E. A.; Gillies, R. J.; Hruby, V. J. Heterobivalent ligands crosslink multiple cell-surface receptors: the human melanocortin-4 and delta-opioid receptors. *Angew. Chem., Int. Ed.* **2008**, *47* (9), 1685−1688. (b) Krchnak, V.; Vagner, J.; Lebl, M. Noninvasive continuous monitoring of solid-phase peptide synthesis by acid-base indicator. *Int. J. Pept. Protein Res.* **1988**, *32* (5), 415−416. (c) Krchnak, V.; Vagner, J. Color-monitored solid-phase multiple peptide synthesis under low-pressure continuous-flow conditions. *Pept. Res.* **1990**, *3* (4), 182−193.

(27) (a) Metzger, J. W.; Wiesmuller, K. H.; Jung, G. Synthesis of N alpha-Fmoc protected derivatives of *S*-(2,3-dihydroxypropyl)-cysteine and their application in peptide synthesis. *Int. J. Pept. Protein Res.* **1991**, *38* (6), 545−554. (b) Reichel, F.; Roelofsen, A. M.; Geurts, H. P. M.; Hämäläinen, T. I.; Feiters, M. C.; Boons, G.-J. Stereochemical dependence of the self-assembly of the immunoadjuvants Pam3Cys and Pam3Cys-Ser. *J. Am. Chem. Soc.* **1999**, *121* (35), 7989−7997.

(28) Guevara-Patino, J. A.; Engelhorn, M. E.; Turk, M. J.; Liu, C.; Duan, F.; Rizzuto, G.; Cohen, A. D.; Merghoub, T.; Wolchok, J. D.; Houghton, A. N. Optimization of a self antigen for presentation of multiple epitopes in cancer immunity. *J. Clin. Invest.* **2006**, *116* (5), 1382−1390.
(29) Schindler, U.; Baichwal, V. R. Three NF-kappa B binding sites in the human E-selectin gene required for maximal tumor necrosis factor alpha-induced expression. *Mol. Cell. Biol.* **1994**, *14* (9), 5820−5831.
(30) Handl, H. L.; Vagner, J.; Yamamura, H. I.; Hruby, V. J.; Gillies, R. J. Lanthanide-based time-resolved fluorescence of in cyto ligand−receptor interactions. *Anal. Biochem.* **2004**, *330* (2), 242−250.
(31) Appay, V.; Rowland-Jones, S. L. The assessment of antigen-specific CD8+ T cells through the combination of MHC class I tetramer and intracellular staining. *J. Immunol. Methods* **2002**, *268* (1), 9−19.